

The Chatt–Dewar–Duncanson Model Revisited: X-ray, DFT and NMR Studies of Rhodium-Alkene Binding—Deviations from Structural Ideality

David W. Price,^[b] Michael G. B. Drew,^[b] King Kuok (Mimi) Hii,^[a] and John M. Brown*^[a]

Abstract: An analysis has been made of deviations from ideal centrosymmetric bonding of alkenes to transition metals in square-planar complexes. Three separate approaches have been employed. Firstly, the geometries obtained for a series of X-ray crystal structures of monosubstituted rhodium-alkene complexes have been obtained. Secondly, DFT computations on closely related rhodium-alkene complexes are reported. Thirdly, the data have been augmented by recourse to the crystal structure search and retrieval file (CSSR) database to retrieve the X-ray data for

square-planar ethene and monosubstituted alkene complexes. The results obtained from these analyses provide a consistent picture. Two distortions from ideality are important: twisting of the alkene about the axis between the metal (M) and the alkene centroid and rolling of the alkene around a cylinder enclosing the metal, such that the two C–M

bonds remain equal in length. The presence of both of these is verified through both X-ray structure determinations and DFT calculations. For the rolling distortion, there is a relationship between the electronic character of the substituent on the alkene and the direction of roll. The net effect of this is to place the more nucleophilic carbon of the alkene closer to the square plane. The significance of this for the regiochemistry of the Heck reaction is briefly discussed.

Keywords: alkene complexes • density functional calculations • pi interactions • rhodium • structure elucidation

Introduction

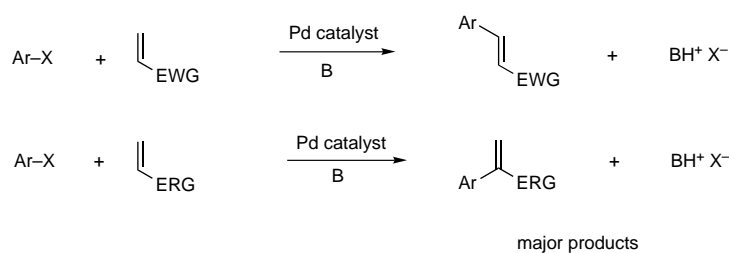
One of the central paradigms in organometallic chemistry is the model of metal–alkene binding, first described by Dewar and given experimental context by Chatt and Duncanson.^[1] This model emphasises the dual nature of the bond with contributions from both alkene donor and alkene acceptor through the respective involvement of empty or filled metal d orbitals. Not surprisingly, the precise nature of this bond has been the subject of many theoretical and experimental studies.^[2] Since coordination of an alkene and subsequent reactions of the resulting complex to make new bonds to carbon form the basis of a substantial sector of homogeneous catalysis, this work has practical importance. Indeed, the recognition of prochiral alkenes by enantiomerically pure transition metal (TM) complexes is central to asymmetric catalysis. A recent comprehensive review has considered the

stereochemical aspects of the structure and chemistry of the TM–alkene bond.^[3] Most discussion assumes a model of coordination with the alkene symmetrically bound, tacitly or otherwise. This becomes significant when the complex is formally square planar with the alkene occupying a single coordination site; the vector of the C–C bond is orthogonal to the coordination plane and, ideally, is bisected by it. The purpose of the present paper is to explore the extent to which reality differs from this ideal and, in particular, whether the variations that occur follow predictable patterns. Our interest arises in part from the observed regioselectivity of the Heck reaction, which varies for monosubstituted alkenes according to Scheme 1.^[4] The control is particularly evident when a cationic Pd catalyst is involved, that is, for the case when X = OTf. Theoretical models for the migration step indicate that the alkene rotates into the coordination plane prior to C–C bond formation and that the sense of rotation will define the outcome of the reaction.^[5] If the alkene is coordinated unsymmetrically this could lead to a predisposition towards one of the two possible products.

MO considerations: A classic paper on metal–alkene coordination by Eisenstein and Hoffmann uses the extended Hückel approach.^[6] In the course of the work they consider the trajectory for nucleophilic attack on a coordinated alkene. Part of the activation process involves asymmetric movement

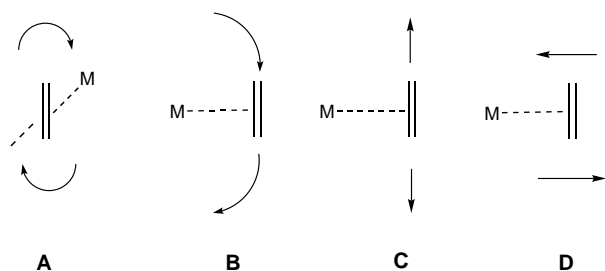
[a] Dr. J. M. Brown, Dr. K. K. (Mimi) Hii
Dyson Perrins Laboratory, University of Oxford
South Parks Road, Oxford, OX1 3QY (UK)
Fax: (+44)1865-275674
E-mail: bjm@ermine.ox.ac.uk

[b] Dr. D. W. Price, Prof. M. G. B. Drew
Department of Chemistry, The University, Whiteknights
Reading, RG6 6AD (UK)
Fax: (+44)118-931-6331
E-mail: m.g.b.drew@reading.ac.uk



Scheme 1. The regiochemistry observed in Heck reactions with cationic palladium catalysts.

of the alkene of the type observed in the X-ray structures discussed below. For the model reaction of $[\text{Fe}(\text{CO})_4(\text{C}_2\text{H}_4)]^{2+}$ with a hydride ion, this slippage makes a positive contribution to the energy barrier, because the LUMO of the alkene becomes more localised on the reacting carbon as the degree of distortion increases, giving a positive overlap population of H^- with $\pi^*_{\text{C-C}}$. Analysis of the geometry of coordinated alkenes was refined later^[7] in the context of bis-alkene complexes, especially $[(\text{alkene})_2\text{Rh}(\text{acac})]$. Four pathways for deviation from ideality were considered. Each one maintains C_2 symmetry in the cited case and is adapted here to a single alkene–metal bond (Scheme 2). Deviation **A** is the rotation of the alkene about the axis defined by the M–alkene



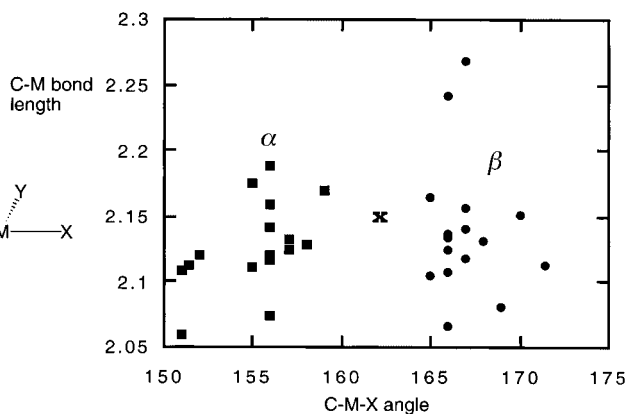
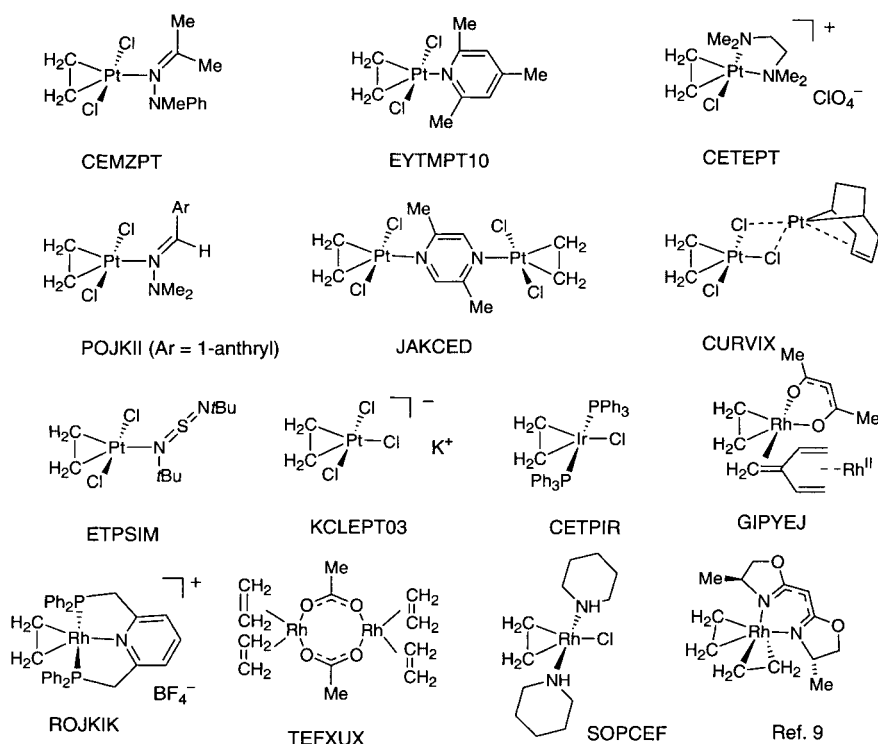
Scheme 2. The possible distortions for a symmetrically disposed dihapto-alkene metal bond: twisting **A**, rolling **B**, translating **C** and rocking **D**.

mid-point. Deviation **B** is the rolling movement of the alkene on the surface of a cylinder centred on M, for which the direction of the projection of the rhodium–alkene mid-point vector onto the square plane and all the rhodium–alkene bond lengths stay constant. Deviation **C** is the translation of the alkene perpendicular to the plane that is defined by M and non-alkene ligands. Finally, deviation **D** is the rocking of the alkene whilst maintaining its mid-point in the square plane and retaining the orthogonal relationship between the C–C bond and the square plane. In the specific case quoted, extended Hückel calculations showed that the trend in energetics for the four processes is $\mathbf{D} > \mathbf{C} \gg \mathbf{A} > \mathbf{B}$, with the low-energy processes **A** and **B** almost equivalent at small displacements. Further work in this system, which included nonbonded interactions between the chiral ligand and bound ethene molecules by means of molecular mechanics, endorsed the conclusion that distortion **B** is energetically most favoured and predicted the extent of distortion observed in the crystal structure to within 0.5° .^[8] On energetic grounds, distortions **C** and **D** are not considered further in this discussion.

Evidence from crystallography:

We examined the crystal structure search and retrieval file (CSSR) database^[9] to retrieve the structures of all square-planar η^2 -ethene complexes and all monosubstituted alkene variants. Among the simple η^2 -ethene complexes, there are 31 relevant Pt structures out of a total of 44; of the rest 11 are Rh complexes with just one representative from Ir chemistry and one from Pd. Among the monosubstituted alkene complexes there is an even greater dominance of Pt structures, with 25 out of a total of 28; the remainder comprises one Pd and two Rh complexes. The objective was to discover variations in coordination geometry and, in particular, to correlate any asymmetric displacements of the alkene relative to the coordination plane. cursory examination indicated that the distortion indicated by **B** in Scheme 2 is frequently significant. For the η^2 -ethene complexes, a measure of the extent of this distortion was defined by comparing the two angles subtended at the metal by the bonds from the metal to the alkene and its *trans* substituent (Scheme 3). If the variation in these was greater than 6° , the X-ray structure and the discussion in the original paper were further scrutinised. For the resulting eleven structures $\text{C}\alpha\text{-M}$ and $\text{C}\beta\text{-M}$ bond lengths were plotted against the C–M–X angle. Within experimental error the two bond lengths were comparable across the range of complexes, indicating that distortion **C** does not make a substantial contribution to nonideality.^[10] Interestingly, the most accurate structure determination for Zeise's salt is by neutron diffraction,^[11] and places the structure within our definition of distorted alkene complexes. The centroid of the alkene is 0.22 \AA out of the coordination plane. Neutron inelastic scattering indicates a large-amplitude rotational oscillation of the ethene.^[12] Among other examples, the structure containing a bis-oxazoline ligand shows considerable rolling distortion that results from nonbonded interactions of the ethene with this ligand (Scheme 3).^[7]

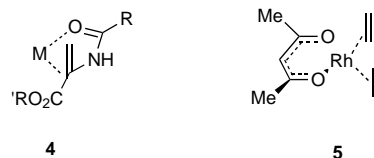
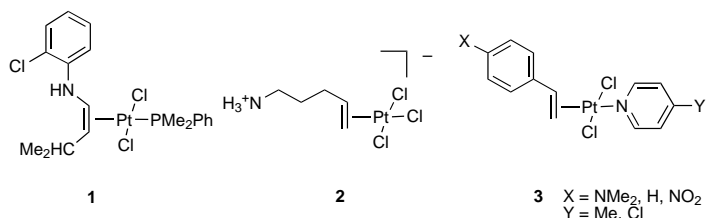
Much discussion of departures from ideal coordination geometry accompanies the X-ray structures of the monosubstituted alkene complexes. Applying the same criteria as before, the structures of eleven Pt complexes were examined in detail. In all of these, the bond from Pt to the more substituted carbon was the longer, frequently significantly so (Scheme 4). This indicates that the distortion of type **B** is accompanied by some contribution from type **C**. In nine of the eleven structures, the methylene carbon was closer to the coordination plane than the methine carbon, subtending the smaller angle (i.e., angle α was generally smaller than angle β). The four β -oxyethene structures^[13] form a consistent pattern with the methylene group closest to the coordination plane; the electronic basis for this has already been discussed.^[13a] Lone-pair donation from the oxygen is considered to impart oxonium-ion character to the alkene C–O bond and at the same time σ character is transferred to the C–M bond of the alkene remote from oxygen. In a related case, the *E*-



Scheme 3. C-M-X angles [°] versus C-M bond lengths [Å] for X-ray structures of selected η^2 -ethene complexes (see text). Symbol **x** represents the values for an undistorted complex. The CSSR codons are displayed.

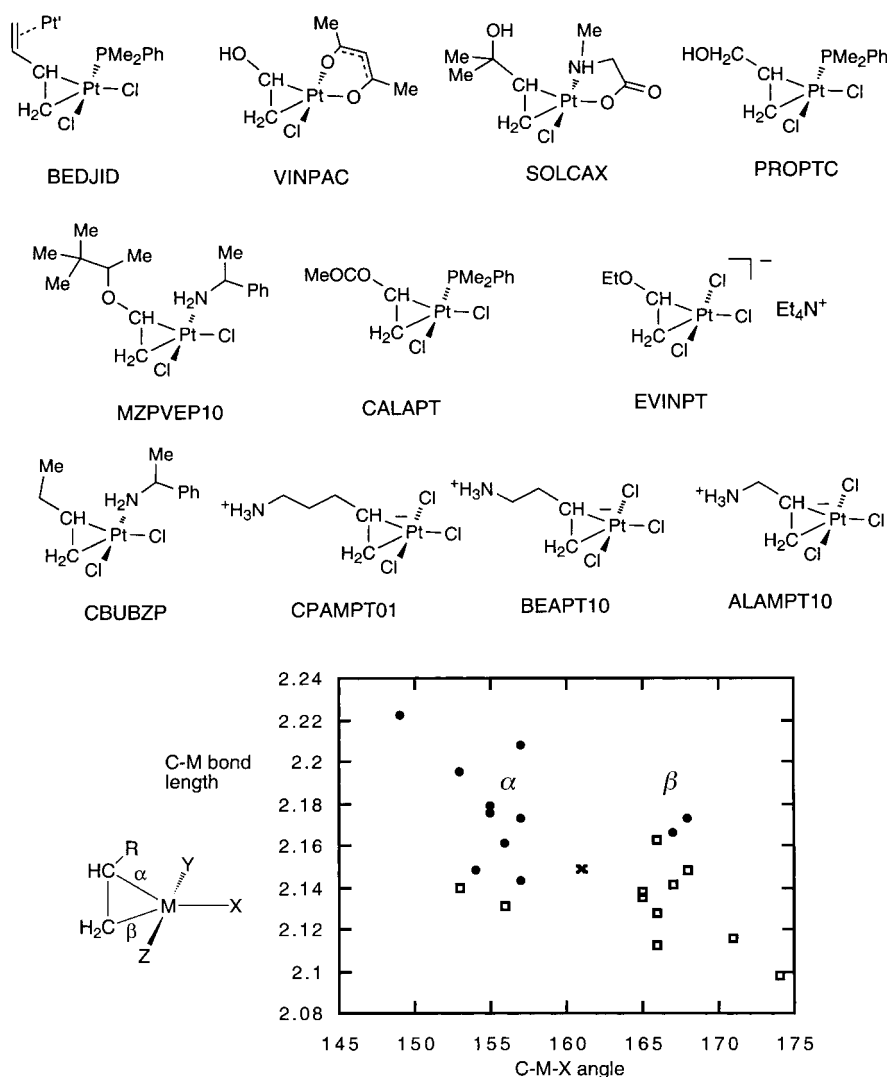
disubstituted enamine complex **1** has the N-terminus of the alkene significantly displaced away from the coordination plane.^[14] The majority of alkyl- or aryl-substituted alkenes

ality shifts towards the square plane, indicated in structure **4**. One non-chelated enamide example indicates the same trend,^[18] but only to a modest extent.



follow a similar pattern. This is not universal, however, the most striking case being that of complex **2** in which two distinct crystal forms (orange or yellow) were obtained with

The aim of the present work was to carry out realistic DFT computations to determine the ground-state structures of a series of alkene complexes and to compare the results with actual X-ray structures. This required a choice of system for which a range of alkenes form stable complexes. The rhodium bis-alkene acetyl acetonates appeared ideal; they are easily



Scheme 4. C-M-X angles [°] versus C-M bond lengths [Å] for X-ray structures of selected η^2 -monosubstituted ethene complexes (see text). The closed circles represent angle α and the open squares angle β as defined. Symbol **x** represents the values for an undistorted complex. The CSSR codons are displayed.

prepared, stable and crystalline. In addition the *dl* isomer of a monosubstituted alkene complex has one C_2 -symmetric rotamer, simplifying computation. DFT calculations are discussed first. The Kohn–Sham formulation of density functional theory provides geometric data for transition metal complexes (amongst others) that are comparable with highly correlated Hartree–Fock calculations^[19] and leads to molecular orbitals with a good physical basis;^[20] thus we have confidence in using these in our analyses.

Computational Details

DFT calculations were carried out with ADF^[21] (v 2.0) on a Silicon Graphics Indigo workstation. The calculations were carried out within the framework of the generalised gradient approximation (GGA) by using the local density functional of Voska, Wilk and Nusair (VWN),^[22] the exchange correction of Becke^[23] and the correlation correction of Perdew.^[24] Frozen core orbitals were used for all atoms other than hydrogen, with the core orbitals for rhodium defined as the 1s, 2s, 2p, 3s, 3p and 3d shells (leaving the 4s, 4p, 5s, 5p and 4d orbitals that contain nine valence and eight subvalence electrons in the neutral atom). The core for all other heavy

atoms was defined as the 1s shell. All calculations were spin restricted and relativistic effects were not included. Model structures were built from the structure of $[(C_2H_4)_2Rh(acac)]$. Substituents were added by using crystal structure data for representative bond lengths, angles and torsions, but no a priori distortion was imposed on the square-planar coordination sphere. The structures were then optimised with respect to their energies by using double- ζ STO basis sets on all atoms initially, and triple- ζ plus polarisation STO basis sets for all atoms for final production runs. These basis sets have been shown to be adequate in describing the structure and bonding of metal carbonyls,^[25] which are among the most computationally demanding class of transition metal compounds. To formalise the deviations from ideality in a coherent set of complexes, the twist angle θ was defined as the rotation of the alkene C–C bond away from orthogonality to the O–Rh–O plane as delineated in Figure 1, model **A**. Likewise ϕ was defined as the angle between the plane formed by the alkene-centroid, Rh atom and the acac oxygen atom *cis* to the alkene and the O–Rh–O plane, as in Figure 1, model **B**. Models **A** and **B** correspond here with the generalised versions shown in Scheme 2.

Results and Discussion

DFT calculations on bis-alkene rhodium complexes

The ethene complex $[(C_2H_4)_2Rh(acac)]$ (5): The X-ray structure of complex **5** has been solved in the older

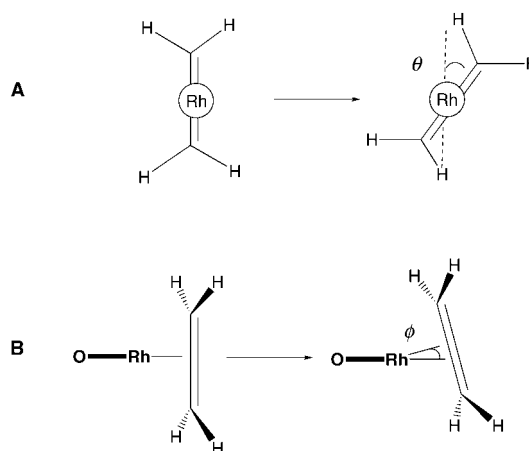


Figure 1. Definitions of the twist angle θ looking down the alkene midpoint–rhodium axis (**A**), and the roll angle ϕ , looking at the molecule in the square plane with the *trans*-acac oxygen, rhodium atom and alkene midpoint all in the plane of the page (**B**).

literature although the coordinates are not available.^[26] Consequently the structure was redetermined Figure 2, and a comparison between this and the DFT minimum energy structure is given in Table 1. Selected bond lengths and angles

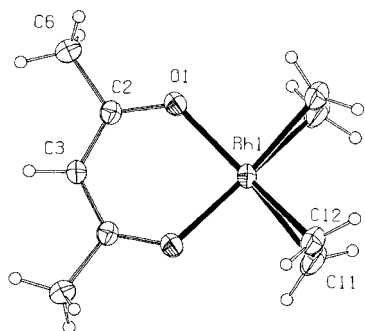


Figure 2. ORTEP structure of complex **5** with ellipsoids at 30% probability.

Table 1. Comparison between bond lengths [Å] and angles [°] from the X-ray data and the DFT minimum energy structure for compound **5**.

	X-ray	DFT
C11–Rh	2.089	2.142
C12–Rh	2.089	2.152
C11–C12	1.392	1.386
O1–Rh	2.035	2.062
C11–Rh–O1	161	161
O1–Rh–O2	92	91
C1–Rh–O2	87	89
H–C–Rh (av)	109	111

from the X-ray data are given in Table 2. The structure of the molecule has crystallographically imposed C_s symmetry although this was not imposed in the DFT calculation. It will be seen that there is a close correspondence between the two structures although heavy-atom bond lengths are about 2–3% shorter in the DFT calculations relative to the experimental values. The degree of rehybridisation is comparable in the two sets of data, when evaluated either from the average H–C–Rh angles of the coordinated alkene or the C=C bond length. Both the X-ray structure and the DFT calculations indicate that the alkene is symmetrically bound in this case, an important factor if the complex is to be used as a model for the understanding of substitution-induced distortions in alkene geometry. A correlation diagram for the parent bis-alkene complex is shown in Figure 3. This reaffirms the notion that metal–olefin bonding is a counter-

Table 2. Bond lengths [Å] and angles [°] in the metal coordination sphere for **5**.

Rh–O1	2.060(4)	Rh–C12	2.142(6)
Rh–C11	2.147(7)	O1#1–Rh–O1	91.0(2)
O1–Rh–C12#	186.7(2)	O1–Rh–C12	160.4(2)
C12#1–Rh–C12	89.1(4)	O1–Rh–C11#	186.0(3)
C12–Rh–C11#	1102.1(3)	O1–Rh–C11	161.4(2)
C12–Rh–C11	37.8(3)	C11#1–Rh–C11	90.9(5)

Symmetry transformations used to generate equivalent atoms: #1 $x, -y+1/2, z$.

poise between donation from occupied metal orbitals ($1b_2, 2b_2$ and $1a_2$) to unoccupied olefin π^* orbitals ($1a_2$ and $1b_2$) and from occupied olefin π orbitals (mainly $1b_1$) to unoccupied metal orbitals (mainly $1b_1$).

Rhodium complexes of monosubstituted ethenes: The good correspondence observed between the structure of the ethene complex and the DFT calculations gave confidence in the approach adopted. A series of computational analyses were carried out for Rh(acac) complexes of monosubstituted alkenes, initially as *dl* rather than *meso* isomers with the substituents placed in *exo*-positions. For the methoxyethene and methyl acrylate complexes two rotameric forms were separately subjected to analysis. In all cases the structure of bound alkene was significantly perturbed from a symmetrical arrangement, and the structural changes were analysed according to the precepts of Scheme 4. The modified structures could be accounted for in terms of the θ and ϕ distortions (**A** and **B** in Figure 1). For all monosubstituted alkenes the optimised structures displayed a combination of both distortions from the idealised geometry, consistent with, but not directly predicted by our earlier studies.^[7] The outcome is shown in Figure 4. In all the *dl-exo* cases the alkene twist is such as to rotate the alkene substituent away from the Rh(acac) plane; this sense is consistent with the reduction of

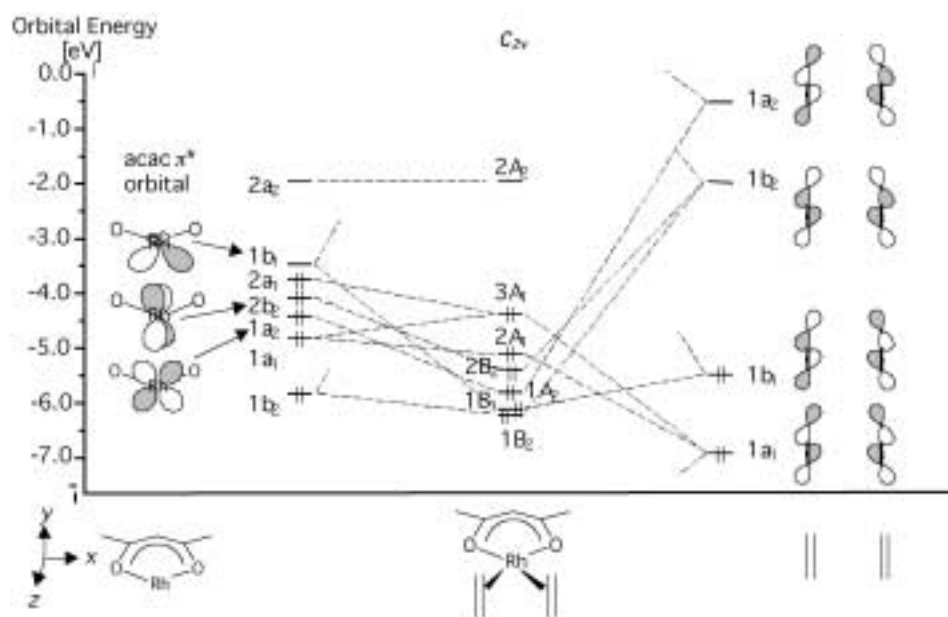


Figure 3. Orbital correlation diagram derived from DFT computation of the minimum energy structure of the parent complex **5**.

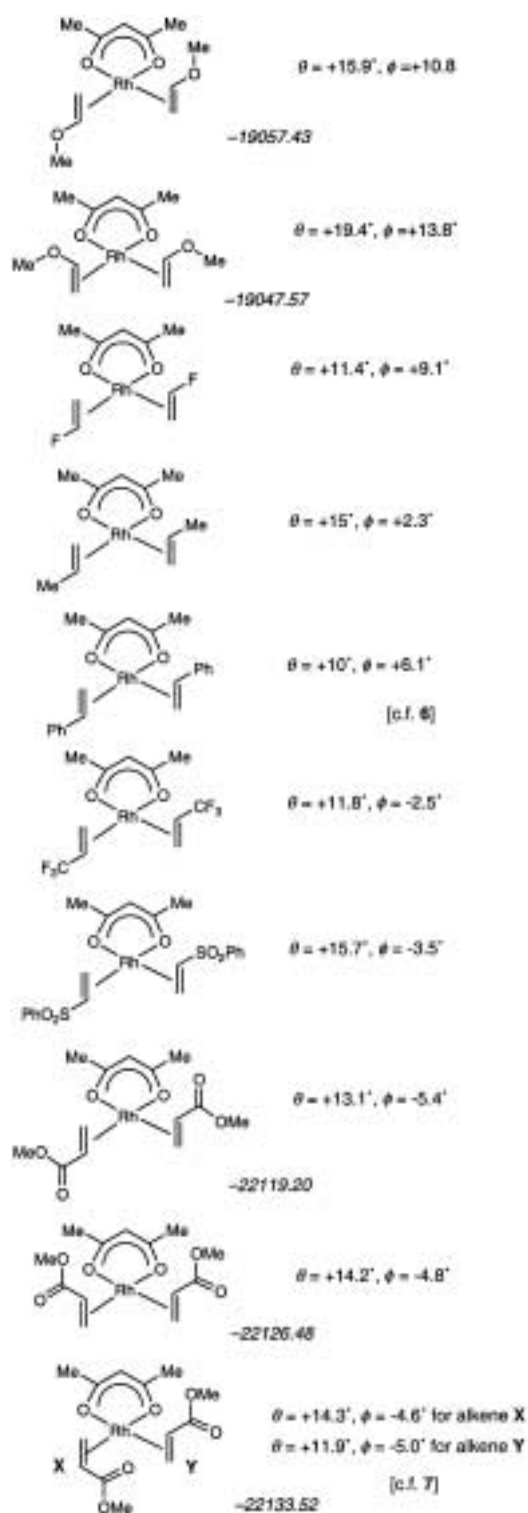


Figure 4. The DFT-computed minimum energy structures for a range of monosubstituted complexes of the form $[(\text{alkene})_2\text{Rh}(\text{acac})]$. Binding energies are italicised under the relevant structures. The values of the twist angle θ and the roll angle ϕ as defined in Figure 1 are given. For the DFT calculation on the bis(ethene) complex reported here, C_{2v} symmetry was imposed, for all others c_2 symmetry was imposed.

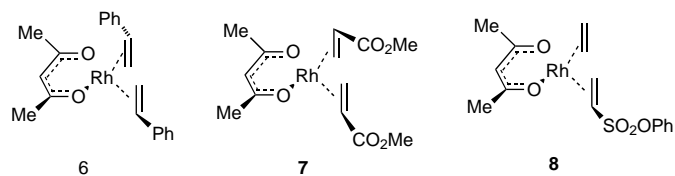
nonbonded interactions between the substituent and the proximate oxygen atom of $\text{Rh}(\text{acac})$.

Consider the complexes with alkenes carrying an electron-donor substituent first, including the bis-fluoroethene com-

plex. Classification of fluorine as an electron-donating substituent implies an important contribution from π donation that outweighs its σ^- character. For all complexes in this class the unsubstituted carbon of the bound alkene is closer to the coordination plane, the extent of which varies with the substituent. Conversely, the methine carbon is more distant from the coordination plane, Π . The most striking case is methoxyethene, in which the extent of lateral displacement of the alkene centroid from the square plane is in accord with the observations already discussed for related Pt-monoalkene XR structures.^[10] The rotameric forms of the complex with the vinyl ether entity in *transoid* or *cisoid* conformation provide similar results. The preferred ground-state conformation of an alkoxyalkene is *cisoid*,^[27] but the DFT calculations place the *transoid* conformer 10 kJ mol^{-1} lower in energy, in line with the X-ray structure of a vinyl ether complex [EVINPT] cited in Scheme 4. DFT calculations also place the styrene complex in the same category with a positive value of ϕ , implying that the methylene carbon of the alkene is closer to the coordination plane than the methine carbon. The distortion in this case may be purely due to steric interactions between the bulky phenyl ring and the acac group. The structure reproduces the main features of the X-ray determination, but exaggerates their deviation from ideality (vide infra). In contrast, for the four DFT calculations on complexes that contain electron-deficient alkenes, the calculated distortion displaces the substituted carbon towards the plane Π , and ϕ is negative. The extent of shift of the centroid is rather less here than for the electron-rich alkenes, but the trend is just as clear. For methyl acrylate, there is only a small difference in ground-state energy between the *s-cis* and *s-trans* forms,^[28] although X-ray structures of its η^2 -alkene complexes indicate that the *s-cis* form is favoured.^[29] DFT calculations were carried out for both the *s-cis* and *s-trans* conformers of the symmetrical *dl* isomer. Their structures were similar, with a 7 kJ mol^{-1} difference in favour of the *s-cis* conformer, but when the X-ray structure became available this proved to be the unsymmetrical *meso* form (vide infra). Hence a further computation was carried out for the experimentally observed conformer, which proved to be 7 kJ mol^{-1} more stable than the *s-cis dl* form. The extent of distortion of the double bond according to **B** does not correlate with the electron-withdrawing power of the substituent; the phenylsulfonyl group is a superior electron-withdrawing group to methoxycarbonyl in both σ and σ^- linear free-energy relationship (LFE) series.^[30] This indicates that both electronic and steric factors contribute to the ground-state structure and the extent of deviation can be correlated only approximately with the electron-withdrawing character of the substituent. Although this is intuitively expected—the alkene terminus which forms the better σ bond is shifted towards the square plane—it has not been clearly defined in the literature. The X-ray structures described below reinforce this result.

X-ray structures of bis-alkene rhodium complexes: Aside from the redetermination of the bis-ethene complex, three further structures were solved: bis(phenylethene)rhodium pentane-2,4-dioate (**6**), bis(μ^2 -methylpropenoate)rhodium pentane-2,4-dioate (**7**) and ethene(phenylsulfonyloxyeth-

ene)rhodium pentane-2,4-dioate (**8**). The data collection details are recorded in the Experimental Section.



X-ray structure of bis(phenylethene)rhodium pentane-2,4-dioate (6): In this bis-styrene complex there are two molecules in the asymmetric unit of a centrosymmetric space group with similar structures. Since one of the independent molecules has the alkenes bound *Re, Re* and the other has them bound *Si, Si*, the structure resembles a racemate but small differences between the two molecular parameters makes them distinct. Both molecules exhibit the alkene twist θ anticipated from the DFT calculations, but the alkene is more centrosymmetrically bound in the X-ray structures than in the theoretical model, that is, experimental ϕ values are smaller than calculated values. Indeed, within experimental error, the centroid of the Rh–alkene bond is in the square plane in both molecules. In the two molecules of the asymmetric unit, the aryl rings are differentially twisted out of the plane of conjugation with the coordinated alkene, the dihedral angle $C_{ortho}-C_{ipso}-C_{\alpha}-C_{\beta}$ varying between 10 and 20°; for the DFT structure the corresponding dihedral angle is 9°. The ORTEP diagram is recorded in Figure 5 along with a comparison of the X-ray and

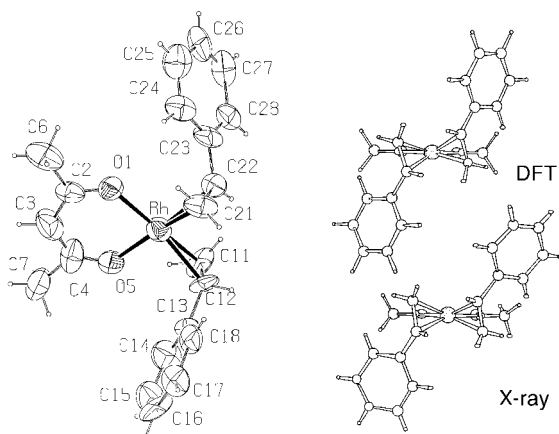


Figure 5. The structure of complex **6** with ellipsoids at 30% probability. The inset shows a comparison of elevation views of the XR and DFT structures.

DFT structures viewed in elevation and the key bond lengths and angles from the X-ray data are collected in Table 3. An X-ray structure of bis-styrene $PtCl_2$, which exists as the unsymmetrical *dl* form, has been reported.^[31]

X-ray structure of bis(η²-methylpropenoate)rhodium pentane-2,4-dioate (7): Crystallisation of the product formed by displacing ethene from $[(C_2H_4)_2Rh(acac)]$ with methyl acrylate led to a complex obtained as orange crystals whose structure is shown in Figure 6 (top) (Table 4 gives a comparison of the X-ray and DFT data for the C–Rh–O angles), with bond lengths and angles recorded in Table 5. This defines the

Table 3. Bond lengths [Å] and angles [°] in the metal coordination sphere for **6**.

	Molecule 1	Molecule 2
Rh–O5	2.07(2)	2.01(2)
Rh–C21	2.11(3)	2.17(3)
Rh–C22	2.18(2)	2.19(2)
Rh–O1	2.18(2)	2.15(2)
Rh–C11	2.21(3)	2.24(3)
Rh–C12	2.28(3)	2.16(2)
O5–Rh–C21	164.5(9)	159.8(9)
O5–Rh–C22	158.9(7)	162.7(10)
C21–Rh–C22	36.5(9)	37.5(9)
O5–Rh–O1	89.8(8)	90.1(7)
C21–Rh–O1	84.6(9)	82.9(8)
C22–Rh–O1	95.2(10)	94.8(9)
O5–Rh–C11	82.7(9)	81.4(8)
C21–Rh–C11	106.8(10)	110.1(9)
C22–Rh–C11	86.1(10)	89.2(9)
O1–Rh–C11	161.1(8)	162.3(9)
O5–Rh–C12	95.5(9)	91.7(8)
C21–Rh–C12	85.9(8)	88.0(9)
C22–Rh–C12	85.8(11)	90.0(10)
O1–Rh–C12	162.3(7)	157.8(8)
C11–Rh–C12	36.6(8)	39.0(10)

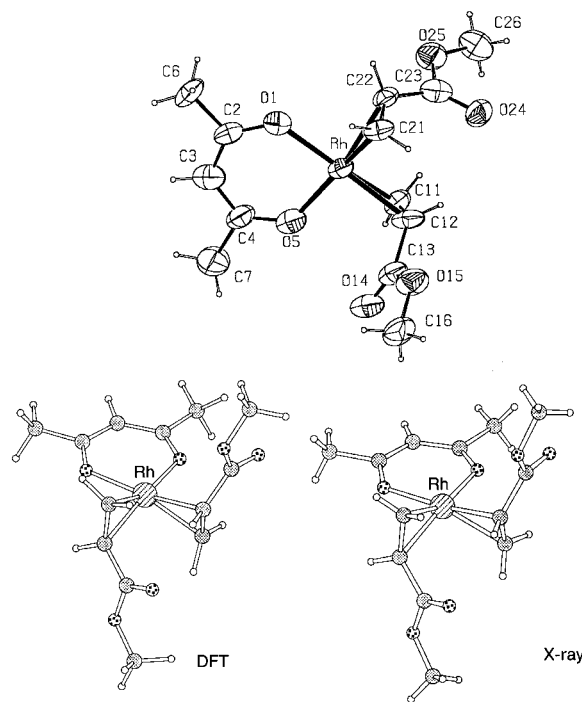


Figure 6. Top: The structure of complex **7** with ellipsoids at 30% probability. Bottom: Comparison of XR and DFT structures for the unsymmetrical *meso*-isomer.

crystalline complex as the unsymmetrical *meso* isomer, but with one alkene coordinated in *exo* and one in *endo* fashion. With this in hand, a direct comparison between the geometries of a calculated structure and an observed structure embracing an electron-withdrawing alkene was possible, and an excellent correspondence is found. Figure 6 (bottom) demonstrates the close similarity between the experimental and computational structures. The main features of the X-ray structure are reproduced: the greater degree of twist distortion Δ for the alkene with the *exo* ester, the shift of the

Table 4. Comparison of the X-ray and DFT data for the C–Rh–O angles [°] for compound **7**.

	DFT	X-ray
<i>endo</i> -H ₂ C–Rh–O	155	156
<i>endo</i> -(OC)C–Rh–O	165	163
<i>exo</i> -H ₂ C–Rh–O	156	154
<i>exo</i> -(OC)C–Rh–O	166	169

Table 5. Bond lengths [Å] and angles [°] in the metal coordination sphere for **7**.

Rh1–O1	2.037(11)	Rh1–O5	2.074(12)
Rh1–C21	2.15(2)	Rh1–C11	2.15(2)
Rh1–C12	2.16(2)	Rh1–C22	2.19(2)
O1–Rh1–O5	88.8(4)	O1–Rh1–C21	86.4(5)
O5–Rh1–C21	156.5(5)	O1–Rh1–C11	153.9(6)
O5–Rh1–C11	82.5(6)	C21–Rh1–C11	110.8(7)
O1–Rh1–C12	168.6(5)	O5–Rh1–C12	94.8(6)
C21–Rh1–C12	86.0(7)	C11–Rh1–C12	37.5(6)
O1–Rh1–C22	84.5(5)	O5–Rh1–C22	163.6(5)
C21–Rh1–C22	38.0(6)	C11–Rh1–C22	97.1(6)
C12–Rh1–C22	94.7(6)		

methoxycarbonyl-bearing carbon towards the square plane in both cases and the *cisoid* conformation of the $\alpha\beta$ -unsaturated carbonyl groups. The C–Rh bond lengths do not vary widely; the DFT calculations predict longer C–Rh bonds to the methine carbon than the methylene carbon, and this is realised experimentally for the *endo* alkene.

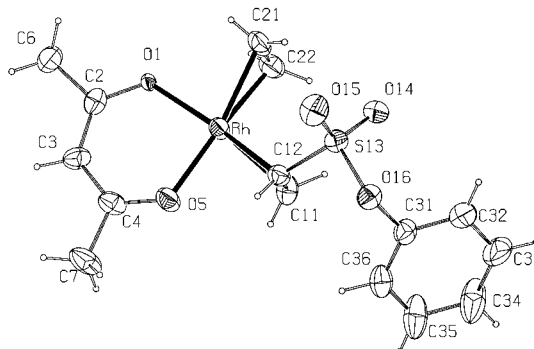
X-ray structure of ethene(phenylsulfonyloxyethene)rhodium pentane-2,4-dioate (8): Although it is not one of the structures considered in the DFT calculations, the availability of good quality crystals of the phenylsulfonyloxy complex and the established electron-withdrawing character of the substituent^[32] encouraged us to study the structure. The result is encouraging, since it fits nicely with expectation and even provides an internal calibration. Within error, the ethene is centrosymmetrically coordinated and the substituted alkene is not. There is a small degree of twist **A**, but also a significant lateral displacement according to **B** (Figure 1) such that the substituted carbon is closer to the coordination plane; the (SO₂)C–Rh–O angle is 164.1(2)° and the (H₂)C–Rh–O angle is 154.1(2)°. The two C–Rh bond lengths for the alkene are comparable (2.094(5), 2.100(5) Å) and both are significantly shorter than the ethene C–Rh bond lengths (2.138(5), 2.148(5) Å). The alkene C=C bond is longer than the ethene C=C bond at 1.430(7) Å versus 1.372(8) Å. The structure is shown in Figure 7 and selected bond lengths and angles are given in Table 6.

Conclusion

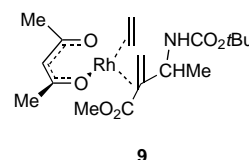
Taking the new X-ray structures together and applying the same criteria as was used for CSSR-acquired structures, a consistent pattern arises (Scheme 5). In all cases the substituted carbon lies closer to the coordination plane, in contrast

Table 6. Bond lengths [Å] and angles [°] in the metal coordination sphere for **8**.

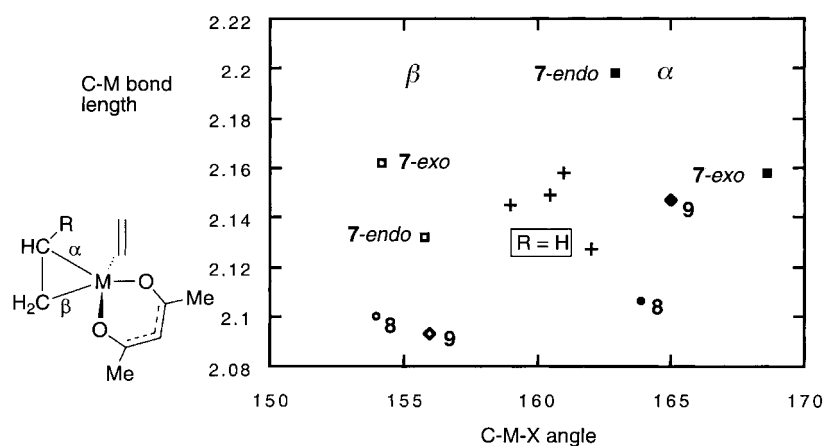
Rh–O5	2.030(4)	Rh–O1	2.038(4)
Rh–C11	2.094(5)	Rh–C12	2.100(5)
Rh–C22	2.138(5)	Rh–C21	2.148(5)
O5–Rh–O1	91.51(13)	O5–Rh–C11	84.7(2)
O1–Rh–C11	154.1(2)	O5–Rh–C12	81.7(2)
O1–Rh–C12	164.1(2)	C11–Rh–C12	39.9(2)
O5–Rh–C22	160.9(2)	O1–Rh–C22	86.0(2)
C11–Rh–C22	89.2(2)	12–Rh–C22	105.0(2)
O5–Rh–C21	161.2(2)	1–Rh–C21	83.8(2)
C11–Rh–C21	107.2(2)	12–Rh–C21	98.1(2)
C22–Rh–C21	37.1(2)		

Figure 7. The structure of complex **8** with ellipsoids at 30% probability.

to most of the data accumulated in Scheme 4. Complex **9** is included for completeness and provides an additional pair of data points from the η^2 -ethene coordinates for comparison. This work was originally motivated by considerations of the



regiochemistry of metal-catalysed reactions of alkenes and the interpretation of trends. For example, in the Heck reaction of aryl or vinyl triflates with substituted alkenes there appears to be an electronic influence on the reaction course, namely, a preference for the new C–C bond to be formed at the more electron-rich of the two unsaturated centres. The reaction mechanism indicated by DFT calculations^[5] involves rotation of an orthogonal alkene into the square plane followed by C–C bond formation. Depending on the direction of rotation, coupling will occur to either *Ca* or *Cβ*. The present observations accord well with literature experimental results if a least-motion pathway is considered, and alkene rotation occurs towards the Pd–electrophile bond. This is especially true when cationic intermediates (normally the case with triflate electrophiles) are employed; the new C–C bond is formed at the alkene terminus that carries the more electron-releasing substituents. In all cases considered here the outcome is the same. An electron-releasing substituent on an alkene shifts away from the coordination plane, whilst an electron-withdrawing substituent shifts towards the coordination plane. The first case had previously been recognised and



Scheme 5. C-M-X angles [°] versus C-M bond lengths [Å] for X-ray structures of complexes **7**, **8** and **9**. Closed symbols represent angle α , open symbols represent angle β and crosses represent either angle of a coordinated ethene.

exemplified, but the second had not. Hence, a more complete picture of geometry variation in coordinated alkenes and the underlying causes is now on hand. In conclusion, a note of caution is warranted. The energy of displacement of a coordinated alkene along either path **A** or path **B** (Figure 1) is small, and for many of the structures cited may be of the same order as crystal packing forces.^[12]

Experimental Section

Crystallographic data: Crystal data are given in Table 7, together with refinement details. Data for all four crystals were collected with Mo_{K α}

Table 7. Crystal data and structure refinement details for compounds **5**, **6**, **7** and **8**.

	5	6	7	8
formula	[Rh(acac)(C ₂ H ₄) ₂]	[Rh(acac)(CH ₂ CHPh) ₂]	[Rh(acac)(CH ₂ CHCO ₂ CH ₃) ₂]	[Rh(acac)(C ₂ H ₄)(CH ₂ CHSO ₃ Ph)]
empirical formula	C ₉ H ₁₅ O ₂ Rh	C ₂₁ H ₂₅ O ₂ Rh	C ₁₃ H ₁₉ O ₆ Rh	C ₁₃ H ₁₉ O ₃ RhS
M _w	258.12	410.30	374.19	414.27
T [K]	293(2)	293(2)	293(2)	293(2)
λ [Å]	0.71073	0.71073	0.71073	0.71073
crystal system	orthorhombic	monoclinic	monoclinic	monoclinic
space group	<i>Pnma</i>	<i>P2₁/c</i>	<i>P2₁/n</i>	<i>P2₁/n</i>
Z	4	4	4	4
a [Å]	7.775(9)	8.429(7)	10.960(11)	8.882(9)
b [Å]	14.506(12)	35.45(3)	9.362(9)	9.615(10)
c [Å]	9.232(9)	13.507(7)	16.015(14)	19.38(2)
β [°]	90	95.23(1)	91.22(1)	92.68(1)
V [Å ³]	1041	4019	1643	1653
ρ_{calcd} [Mgm ⁻³]	1.653	1.356	1.513	1.646
μ [mm ⁻¹]	0.858	1.601	1.058	1.173
F(000)	524	1680	760	832
crystal size [mm]	0.15 × 0.20 × 0.25	0.25 × 0.25 × 0.15	0.25 × 0.30 × 0.30	0.25 × 0.30 × 0.30
θ range [°]	2.81–24.98	2.68–25.02	2.52–25.28	2.37–25.84
index ranges	0 ≤ h ≤ 9 –17 ≤ k ≤ 17 –9 ≤ l ≤ 10	0 ≤ h ≤ 9 –41 ≤ k ≤ 41 –10 ≤ l ≤ 10	0 ≤ h ≤ 12 –9 ≤ k ≤ 10 –18 ≤ l ≤ 18	0 ≤ h ≤ 10 –10 ≤ k ≤ 11 –23 ≤ l ≤ 23
reflections collected	2959	5191	4862	4765
independent reflections [R(int)]	913 [0.0301]	3140 [0.0821]	2696 [0.0879]	2842 [0.0235]
data/restraints/parameters	913/4/76	3133/16/475	2696/6/201	2842/7/223
GOOF on F ²	0.851	0.779	1.090	1.075
R1 [I > 2σ(I)]	0.0486	0.0863	0.1139	0.0407
wR2 [I > 2σ(I)]	0.1307	0.2314	0.2729	0.1150
R1 (all data)	0.0519	0.1623	0.1602	0.0448
wR2 (all data)	0.1370	0.3054	0.3025	0.1208
largest diff. peak/hole [e Å ⁻³]	1.076/–1.958	0.557/–0.628	0.878/–1.525	1.370/–1.311

radiation with the MARresearch Image Plate System. The crystals were positioned at 75 mm from the image plate. 95 frames were measured at 2° intervals with a counting time of 2 mins. Data analysis was carried out with the XDS program.^[33] All structures were solved using direct methods with the SHELXS-86 program.^[34] All non-hydrogen atoms were refined with anisotropic thermal parameters. The hydrogen atoms were included in geometric positions apart from those on the ethene carbon atoms, which were allowed to refine independently. All four structures were then refined on F² using SHELXL-93.^[35] Crystallographic data (excluding structure factors) for the structures reported in this paper have been deposited with the Cambridge Crystallographic Data Centre as supplementary publication

no. CCDC-145506–144509. Copies of the data can be obtained free of charge on application to CCDC, 12 Union Road, Cambridge CB2 1EZ, UK (fax: (+44) 1223-336-033; e-mail: deposit@ccdc.cam.ac.uk). Calculations were carried out on a Silicon Graphics R4000 Workstation at the University of Reading.

Preparation and characterisation of rhodium complexes: [(acac)Rh(C₂H₄)₂] was prepared as previously published^[36] by the reaction of potassium acetylacetonate with [Rh(C₂H₄)₂Cl]₂. Replacement of ethene by other alkenes was carried out by the procedure outlined below: The alkene (0.1 mL) was added to a solution of [(acac)Rh(C₂H₄)₂] (0.1 g, 0.39 mmol.) in diethyl ether (1 mL), whereupon gas evolution was observed. The reaction mixture was stirred for 10 min before evaporation to dryness under reduced pressure. Petroleum ether (30–40%, 5–10 mL) was added to the residue at –78 °C, and the product was obtained as a yellow solid,

which was filtered off and washed with cold solvent. In all cases the NMR spectra were fluxional at room temperature, with complex ¹H spectra at lower temperatures, presumably due to a mixture of interchanging rotamers or diastereomers.

Bis(η^2 -methylpropenoate) complex 6: Yield 113 mg, 78%; IR (KBr): $\bar{\nu}$ = 1725 (s), 1715 cm⁻¹ (s); for ¹³C NMR spectra see Table 8.

Bis(phenylethene) complex 7: Yield: 103 mg, 65%. elemental analysis calcd (%) for C₂₁H₂₃O₂Rh: C 61.45, H 5.65; found: C 61.4, H 5.4%; for ¹³C NMR spectra see Table 8.

Ethene(phenylsulfonyloxyethene) complex 8: Yield 80%; for ¹³C NMR spectra see Table 8.

Table 8. ¹³C NMR spectra of rhodium alkene complexes **5**, **6**, **7** and **8**.^[a]

	CH ₂	CHY	CH ₃	CH	CO	Others
5 ^[b]	59.6 (12)	–	27.3	99.1	186.4	–
6 ^[c]	49.3(14)	70.1(12)	26.6	98.5	185.5	131.1–122.3, Ph
	53.5 (12)	72.6 (12)	27.1	98.7	185.6	140.4, 140.7, 140.8, C-1
	53.7 (12)	73.5 (12)	27.3	98.9	185.7	
	56.1 (12)	73.9 (12)			185.8	
	56.1 (12)	75.4 (10)				
7 ^[d]	59.8 (12)	58.6 (14)	27.1	99.1	186.1	51.8, 51.9, 52.3, OMe
	61.2 (12)	61.3 (14)	27.2	99.2	186.3	172.6, 172.7, 173.1, CO ₂ Me
	61.6 (12)	61.6 (14)			186.4	
	64.2 (12)	62.5 (14)				
8 ^[e]	52.2 (25)	61.6 (25)	27.0	99.2	186.1	149.6, C-1
	68.1 (13)		27.4		187.0	122.0, 127.0, 129.7, Ph
	69.1 (13)					

[a] Chemical shifts are given in ppm relative to TMS, recorded at 125.7 MHz in CDCl₃. *J*(Rh–C) coupling [Hz] given in parentheses. [b] At 273 K. [c] At 233 K. [d] At 253 K. [e] At 243 K.

Acknowledgement

We thank E.P.S.R.C. for support of Dr. Hii, and the University of Reading for funds for the Image Plate System. Johnson–Matthey kindly provided a loan of rhodium salts. JMB acknowledges an unrestricted research grant from Merck, Inc. with gratitude.

- M. J. S. Dewar, *Bull. Soc. Chim. Fr.* **1951**, C71–C79; J. Chatt, L. A. Duncanson, *J. Chem. Soc.* **1953**, 2939–2947.
- Recently: J. Uddin, S. Dapprich, G. Frenking, B. F. Yates, *Organometallics* **1999**, *18*, 457–465; for an overview see: G. Frenking, N. Fröhlich, *Chem. Rev.* **2000**, *100*, 717–774.
- J. A. Gladysz, B. J. Boone, *Angew. Chem.* **1997**, *109*, 566–602; *Angew. Chem. Int. Ed. Engl.* **1997**, *36*, 550–583.
- W. Cabri, I. Candiani, *Acc. Chem. Res.* **1995**, *28*, 2–7, and references cited therein; A. de Meijere, F. E. Meyer, *Angew. Chem.* **1994**, *106*, 2473–2506; *Angew. Chem. Int. Ed. Engl.* **1995**, *33*, 2379–2411; S. E. Gibson, R. J. Middleton, *Contemp. Org. Synth.* **1996**, *3*, 447–471.
- R. J. Deeth, A. Smith, K. K. Hii, J. M. Brown, *Tetrahedron Lett.* **1998**, *39*, 3229–3232; D. G. Musaev, M. Svensson, K. Morokuma, S. Stromberg, K. Zetterberg, P. Siegbahn, *Organometallics* **1997**, *16*, 1933–1945.
- O. Eisenstein, R. Hoffmann, *J. Am. Chem. Soc.* **1981**, *103*, 4308–4320, and references cited therein.
- J. M. Brown, P. J. Guiry, D. W. Price, M. B. Hursthouse, S. Karalulov, *Tetrahedron: Asymmetry* **1994**, *5*, 561–564.
- D. W. Price, unpublished results.
- D. A. Fletcher, R. F. McMeeking, D. Parkin, *J. Chem. Inf. Comput. Sci.* **1996**, *36*, 746–749; F. H. Allen, O. Kennard, *Chem. Design Automation News* **1993**, *8*, 31–37.
- A referee has suggested that the comparisons might better be made on the basis of the out-of-plane displacement of the alkene carbons from the best plane described by the metal and other directly bonded atoms. We have sampled structural data from Schemes 3 and 4 for this purpose and confirm that the trends in out-of-plane displacement for atoms C_α and C_β in Å parallel those in the corresponding angles α and β as defined [smaller angle corresponds to larger displacement]: For EPTSIM C_α 0.792, α 158°, C_β 0.546, β 166°; for CEMZPT C_α 0.760, α 159°, C_β 0.569, β 165°; for CALAPT C_α 0.984, α 155°; C_β 0.369, β 168°; for PROPTC C_α 0.973, α 155°, C_β 0.388, β 156°.
- R. A. Love, T. F. Koetzle, G. J. B. Williams, L. C. Andrews, R. Bau, *Inorg. Chem.* **1975**, *14*, 2653–2657.
- R. E. Ghosh, T. C. Waddington, C. J. Wright, *J. Chem. Soc. Faraday Trans. 2* **1973**, *69*, 275–281.
- a) F. A. Cotton, J. N. Francis, B. A. Frenz, M. Tsutsui, *J. Am. Chem. Soc.* **1973**, *95*, 2483–2486; b) R. C. Elder, F. Pesa, *Acta Crystallogr. Sect. B* **1978**, *34*, 268–270; c) J. R. Briggs, C. Crocker, W. S. McDonald, B. L. Shaw *J. Organomet. Chem.* **1979**, *181*, 213–221; d) F. Sartori, L. Leoni, *Acta Crystallogr. Sect. B* **1976**, *32*, 145–149.
- A. de Renzi, P. Ganis, A. Panunzi, A. Vitigliano, G. Valle, *J. Am. Chem. Soc.* **1980**, *102*, 1722–1723.
- R. Spagna, L. Zambonelli, *Acta Crystallogr. Sect. B* **1972**, *28*, 2760–2765.
- S. C. Nyburg, K. Simpson, W. Wong-Ng, *J. Chem. Soc. Dalton Trans.* **1976**, 1865–1870.
- For X-ray structures of enamide complexes which demonstrate this structural feature see: A. S. C. Chan, J. J. Pluth; J. Halpern, *Inorg. Chim. Acta* **1979**, *37*, L477–480; A. S. C. Chan, J. J. Pluth, J. Halpern, *J. Am. Chem. Soc.* **1980**, *102*, 5952–5953; N. W. Alcock, J. M. Brown, A. E. Derome, A. R. Lucy, *J. Chem. Soc. Chem. Commun.* **1985**, 575–578; N. W. Alcock, J. M. Brown, P. J. Maddox, *J. Chem. Soc. Chem. Commun.* **1986**, 1532–1534; B. McCulloch, J. Halpern, M. R. Thompson, C. R. Landis, *Organometallics* **1990**, *9*, 1392–1395.
- N. W. Alcock, J. M. Brown, A. P. James, *Acta Crystallogr. Sect. C* **1989**, *45*, 734–736.
- V. Barone, C. Adano, *J. Phys. Chem.* **1996**, *100*, 2094–2099; R. J. Deeth, *J. Chem. Soc. Dalton Trans.* **1993**, 3711–3713.
- “Chemical Applications of Density Functional Theory”, E. J. Baerends, O. V. Gritsenko, R. van Leeuwen, *ACS Symp. Ser.* **1996**, *629*, 20–41; R. Stowasser, R. Hoffman, *J. Am. Chem. Soc.* **1999**, *121*, 3414–3420.
- E. J. Baerends, D. E. Ellis, P. Ros, *Chem. Phys.* **1973**, *2*, 41–51.
- S. H. Vosko, L. Wolk, M. Nusair, *Can. J. Phys.* **1980**, *58*, 1200–1211.
- A. D. Becke, *Phys. Rev. A* **1988**, *38*, 3098–3100.
- J. P. Perdew, *Phys. Rev. B* **1986**, *33*, 8822–8824.
- A. Rosa, A. W. Ehlers, E. J. Baerends, J. G. Snijders, G. T. TeVelde, *J. Phys. Chem.* **1996**, *100*, 5690–5696.
- J. A. Evans, D. R. Russell, *J. Chem. Soc. D* **1971**, 197–198.
- I. S. Ignat'ev, A. N. Lazarev, M. B. Smirnov, M. L. Alpert, B. A. Trofimov, *J. Mol. Struct.* **1981**, *72*, 25–39; J. Liu, S. Niwayama, Y. You, K. N. Houk, *J. Org. Chem.* **1998**, *63*, 1064–1073; D. Bond, P. von R. Schleyer, *J. Org. Chem.* **1990**, *55*, 1003–1013.
- T. Egawa, S. Maekawa, H. Fujiwara, H. Takeuchi, S. Konaka, *J. Mol. Struct.* **1995**, *352*, 193–201; J. I. Garcia, J. A. Mayoral, L. Salvatella, X. Assfeld, M. F. Ruiz-Lopez, *THEOCHEM* **1996**, *362*, 187–197; R. J. Loncharich, T. R. Schwartz, K. N. Houk, *J. Am. Chem. Soc.* **1987**, *109*, 14–23.
- A. Jutand, K. K. Hii, M. Thornton-Pett, J. M. Brown, *Organometallics* **1999**, *17*, 5367–5374, and references cited therein.
- A. J. Gordon, R. A. Ford, *The Chemist's Companion*, Wiley Interscience, New York, **1972**, pp. 144–149.
- A. Albinati, W. R. Caseri, P. S. Pregosin, *Organometallics* **1987**, *6*, 788–793.
- H. Shenhav, Z. Rappoport, S. Patai, *J. Chem. Soc. B* **1970**, 469–476; L. L. Klein, T. M. Deeb, *Tetrahedron Lett.* **1985**, *26*, 3935–3938.
- W. Kabsch, *J. Appl. Crystallogr.* **1988**, *21*, 916–924.
- SHELXS-86: G. M. Sheldrick *Acta Crystallogr. Sect. A* **1990**, *46*, 467–473.
- G. M. Sheldrick, *SHELXL-93, Program for Crystal Structure Refinement*, University of Gottingen, **1993**.
- R. Cramer, *J. Am. Chem. Soc.* **1964**, *86*, 217–221.

Received: April 10, 2000 [F2412]